

## Slit-patterned CoNbZr/Nb/CoNbZr magnetic film for rf noise suppressor

著者	Ikeda Shinji, Kim Ki Hyeon, Yamaguchi Masahiro
journal or publication title	Journal of Applied Physics
volume	97
number	10
page range	10F912-1
year	2005
URL	<a href="http://hdl.handle.net/10097/52045">http://hdl.handle.net/10097/52045</a>

doi: 10.1063/1.1858691

# Slit-patterned CoNbZr/Nb/CoNbZr magnetic film for rf noise suppressor

Shinji Ikeda,<sup>a)</sup> Ki Hyeon Kim, and Masahiro Yamaguchi

Department of Electrical and Communication Engineering, Graduate School of Engineering, Tohoku University, Sendai 980-8579, Japan

(Presented on 10 November 2004; published online 10 May 2005)

In this paper, we discuss the elimination of magnetic closure domains in a micropatterned film in order to have the desired loss generation profile against the operating frequency and describe a demonstration of the rf loss generation profile over a thin-film coplanar transmission line using micropatterned films with various slit designs. It was demonstrated that the micropatterned film causes loss in the transmission line in a narrow frequency band and the loss ratio in the other bands is smaller than in the nonpatterned film we measured. The peak frequency of loss generation is controllable according to the pattern dimension of the magnetic film. This technique is useful as a notch filter for integrated transmission lines. © 2005 American Institute of Physics.

[DOI: 10.1063/1.1858691]

## I. INTRODUCTION

Electromagnetic noise suppressors are currently used in modern information technology (IT) equipment to alleviate intra electromagnetic compatibility (intra-EMC) problems in the low gigahertz-range. They are usually attached to the wiring or transmission line on printed circuit boards, large scale integrated circuits, etc. The physical form of the suppressor is a “sheet” consisting of polymer-embedded ferromagnetic flakes.<sup>1</sup> The sheet dissipates noise energy as ferromagnetic resonance (FMR) losses, and therefore, the sheet suppresses the noise only in the high-frequency range beyond the signal frequency range. In the near future, we expect that thin films will be utilized for the suppressors because of the industrial demand for very thin suppressors.

To meet this expected demand, we have already simulated broadband noise attenuation in the 3–20 GHz range by using CoNbZr thin films.<sup>2,3</sup> Our simulation clarified the possibility of controlling the frequency range of loss generation by micropatterning the film into an array of parallel narrow rectangles separated by slits.<sup>4</sup>

This paper first discusses the elimination of magnetic closure domains in the micropatterned film in order to have the desired loss generation profile against the operating frequency. Then it describes an actual demonstration of the rf loss generation profile over a thin-film coplanar transmission line using the micropatterned films with different slit designs. We believe that our findings in this work would lead to a rf notch filter design.

## II. MICROPATTERNED MAGNETIC FILM

Figure 1 shows the structure of a magnetic thin film with slits.<sup>5</sup> The parallel slits were formed along the easy-axis direction of a magnetic film that had in-plane uniaxial anisotropy. The FMR frequency strongly depends on the demagnetizing factor,  $N_d$ , of the patterned film, as indicated by Eq. (1).  $N_d$  is affected by both the increase in shape anisotropy of the slit-patterned film and the change in the magnetostatic

interaction between neighboring film specimens. This is possible at the cost of static permeability along the hard-axis direction, as indicated by Eq. (2).

$$f_r = \sqrt{(H_k M_s + N_d M_s^2) / \mu_0}, \quad (1)$$

$$\mu_{\text{eff}} = M_s / (H_k + N_d M_s). \quad (2)$$

The relation between the dimension of the patterned magnetic film and permeability has been calculated by the authors<sup>6</sup> using the finite element method. It is necessary to eliminate closure domains at the edge of each slit-patterned magnetic film specimen and to reduce their anisotropy dispersion in order to realize sharp FMR loss generation in the frequency profile of complex permeability. We employed a double-layer structure to suppress the closure domain and domain wall. This is effective for a small anisotropy dispersion.

## III. SAMPLE PREPARATION

The samples were composed of sputtered 0.5- $\mu\text{m}$ -thick CoNbZr magnetic film, 10-nm-thick Nb, and 0.5- $\mu\text{m}$ -thick CoNbZr magnetic film on a glass substrate measuring  $4 \times 4 \text{mm}^2$ . The pattern was created by ion milling. The pattern dimensions of each sample were 28/5, 18/4, 7/4, and 6/5  $\mu\text{m}$  (linewidth/slit width). The samples were annealed twice in a dc field at 400 °C to reduce their anisotropy dispersion, once after deposition and once after patterning.

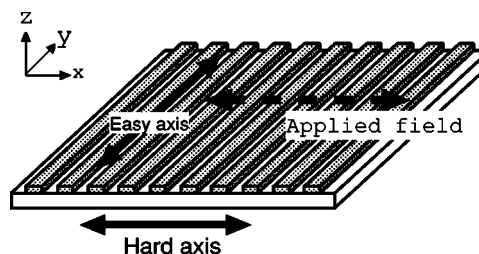


FIG. 1. Schematic view of micropatterned magnetic film.

<sup>a)</sup>Electronic mail: s-ikeda@ecei.tohoku.ac.jp

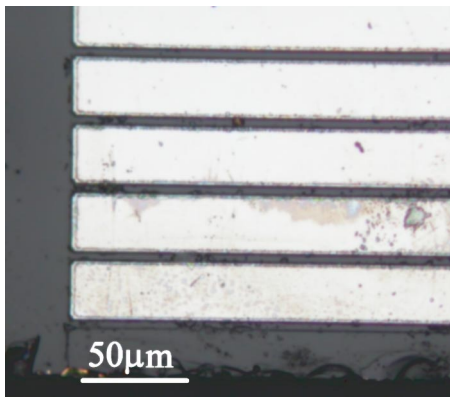


FIG. 2. Photograph of patterned film. The pattern dimension was  $28/5 \mu\text{m}$  (linewidth/slit width).

Figure 2 shows a photo of a sample that had a  $28/5\text{-}\mu\text{m}$  line/slit width. We observed the samples' Kerr images to check the state of the domains. Figure 3 shows Kerr's microscope images. Figure 4 shows the corresponding  $M-H$  curves measured by vibrating-sample magnetometry (VSM).

In Fig. 3, no contrast is visible on the double-layer film, whereas the single-layer film has a closure domain near the edge of each rectangle. It was expected that samples would have no domain wall except the invisible edge curling wall<sup>7</sup> because the  $M-H$  loop of the easy direction of each sample has a step near zero magnetization. That means stability with antiparallel magnetization between the upper layer and bottom layer. From Fig. 4(b), it is clear that a smaller line/space ratio brings a larger effective anisotropy field. For the line/space of  $7/4 \mu\text{m}$ , the effective  $H_k$  is about  $570 \text{ Oe}$ , although the intrinsic anisotropy field was  $8 \text{ Oe}$ .

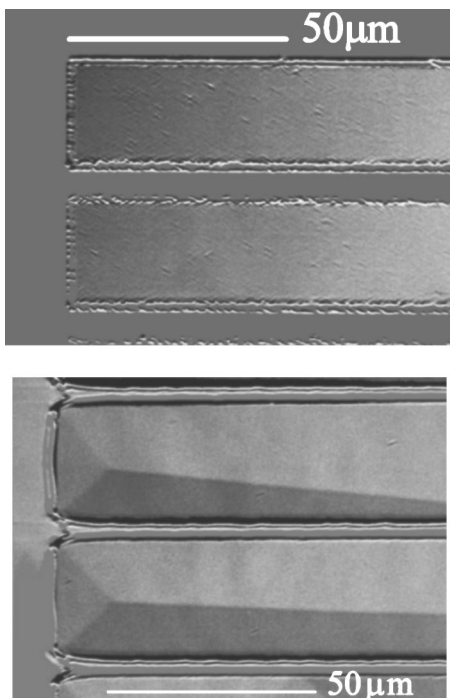


FIG. 3. Kerr microscope image of micropatterned films. (a) Double-layered film and (b) single-layer film.

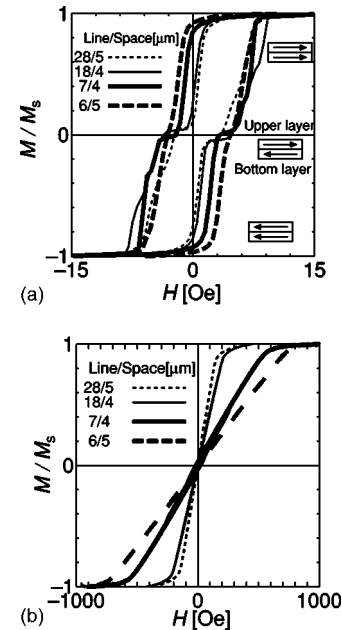


FIG. 4. Measured  $M-H$  curve of micropatterned double-layer films. (a) Easy axis and (b) hard axis.

#### IV. COMPLEX PERMEABILITY

Figure 5 shows the frequency characteristics of complex permeability as measured with a permeameter.<sup>8</sup> The real part of each sample decreases sharply and the imaginary part has a peak at the FMR frequency which was shifted by the enhanced effective  $H_k$ . The real part has a dip around  $3.5 \text{ GHz}$  when static permeability was less than 10. The dip was not caused by the properties of the films because their permeance was smaller than the sensitivity of the permeameter. This result indicates that the FMR loss can cause a few-gigahertz-range loss in the transmission line with a micropatterned magnetic film.

#### V. NOISE SUPPRESSION EXPERIMENTS

Figure 6 shows the frequency profile of the loss ratio of the signal through a  $5.2\text{-mm}$  Cu coplanar transmission line,

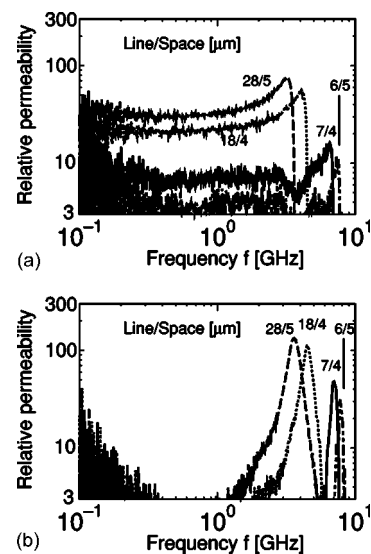


FIG. 5. Measured complex permeability of micropatterned magnetic films. (a) Real part and (b) imaginary part.

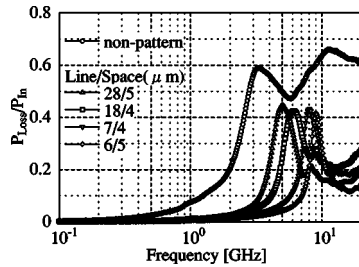


FIG. 6. Power loss of coplanar transmission lines with nonpatterned and slit-patterned magnetic films.

which was put under the magnetic film and a polyimide insulating layer.  $P_{\text{loss}}/P_{\text{in}}$  means the ratio of line loss to the input power of the transmission line [Eq. (3)], and it can be expressed using  $S$  parameters measured by a network analyzer.

$$P_{\text{loss}}/P_{\text{in}} = 1 - (S_{11}^2 + S_{21}^2). \quad (3)$$

In the case of a nonpatterned film,  $P_{\text{loss}}/P_{\text{in}}$  is over 0.4 above 2.5 GHz because the loss is caused by ferromagnetic resonance and the eddy current in the magnetic layer. An electromagnetic simulation has already shown that the first peak is related to FMR. This property is useful for suppressing noise whose frequency is higher than the main signal.<sup>9</sup>

On the other hand, the patterned magnetic film exhibited a low loss ratio at 20 GHz, which resulted from the decrease in eddy current loss in the magnetic layer, and it had a narrow peak. The smaller line/space ratio yielded a higher peak frequency of  $P_{\text{loss}}/P_{\text{in}}$  depending on the FMR frequency. The power loss of the patterned film at 1 GHz (passband frequency) is smaller than that of a nonpatterned film because of the suppression of the eddy current.

## VI. CONCLUSION

It was demonstrated that the micropatterned film generates a loss in the transmission line in a narrow frequency

band and the loss ratio in the other bands is smaller than with the nonpatterned film. The peak frequency of the loss is controllable according to the pattern dimension of the magnetic film. This technique is useful as a notch filter for integrated transmission lines. The micropatterned magnetic films seem effective for ensuring a low insertion loss and controlling the peak frequency of the loss. The possibility of a rf notch filter design was demonstrated by using magnetic films with different slit designs.

## ACKNOWLEDGMENTS

The authors would like to thank Professor Yutaka Shimada (IMRAM Tohoku University) for his discussion with us, Professor Ken-Ichi Arai (RIEC Tohoku University) for making the Kerr observation, and Professor Masashi Sahashi (ECEI Tohoku University) for making the VSM measurements. We also acknowledge the support of the Laboratory for Electric Intelligent Systems RIEC, Tohoku University, the Industrial Technology Institute of the Miyagi prefectural government, the Telecommunications Advancement Organization of Japan, the SCOPE program by Ministry of Public Management Home Affairs, Posts and Telecommunications of Japan, and the Collaboration program between NEC TOKIN Co. and Tohoku University.

<sup>1</sup>S. Yoshida *et al.*, IEEE Trans. Magn. **37**, 2401 (2001).

<sup>2</sup>M. Yamaguchi, K. H. Kim, T. Kuribara, and K.-I. Arai, IEEE Trans. Magn. **38**, 3183 (2002).

<sup>3</sup>K. H. Kim, H. Nagura, S. Ohnuma, M. Yamaguchi, and K.-I. Arai, J. Appl. Phys. **93**, 8002 (2003).

<sup>4</sup>K. H. Kim, S. Ikeda, M. Yamaguchi, and K.-I. Arai, J. Appl. Phys. **93**, 8588 (2003).

<sup>5</sup>M. Yamaguchi *et al.*, IEEE Trans. Magn. **36**, 3495 (2000).

<sup>6</sup>S. Ikeda, K. H. Kim, M. Yamaguchi, K. I. Arai, H. Nagura, S. Ohnuma, and Y. Shimada, J. Magn. Soc. Jpn. **27**, 594 (2003).

<sup>7</sup>J. C. Slonczewski, B. Petak, and B. E. Argyle, IEEE Trans. Magn. **24**, 2045 (1998).

<sup>8</sup>M. Yamaguchi, Y. Miyazawa, K. Kaminishi, and K.-I. Arai, Trans. Magn. Soc. Jpn. **3**, 137 (2003).

<sup>9</sup>K. H. Kim, M. Yamaguchi, S. Ikeda, and K.-I. Arai, IEEE Trans. Magn. **39**, 3031 (2003).